CONTINUUM THEORY OF SINTERING. III. EFFECT OF INHOMOGENEOUS DISTRIBUTION OF PROPERTIES IN COMPACTS AND OF PRESSING CONDITIONS ON THE KINETICS OF SINTERING

V. V. Skorokhod, E. A. Olevskii, and M. B. Shtern

UDC 621.762

It is well known in powder metallurgy practice that the inhomogeneous distribution of a property such as density over the volume of a molding or pressing can have a substantial effect on the kinetics of sintering. This inhomogeneity, and also nonuniformity in the physicochemical composition of a bar lead to inhomogeneous shrinkage and warping during the sintering process, and in some cases to rupture of the working material. Inhomogeneous densification is also produced by pressing conditions which create a different number of degrees of freedom in different parts of the body undergoing sintering.

In order to describe real sintering processes, therefore, it is necessary to take the above factors into account, which requires formulation and solution of the pertinent extremum problems.

Free Isothermal Sintering of an Initially Inhomogeneous Porous Sphere. In studying the influence of an inhomogeneous density distribution on the kinetics of sintering in a general form, it is necessary to simplify the geometry of the object under consideration. With this in mind, we have solved a series of model one-dimensional problems concerning the sintering of a sphere with an initial radially inhomogeneous density distribution.

The density distribution at each moment of sintering is determined by the method of permeable elements – MPE [1]. The volume of the sphere is broken up into N parts, representing concentric spherical layers (Fig. 1). Following the results of [2], the distribution of the radial rate of displacement of material within each element is considered to be linear. Let V_{i-1i} (i = 1, ..., N + 1) be the rate of flow of the material from the (i – 1)-th element to the i-th. Due to symmetry the flow rate at the center of the sphere is

$$V_{01} = 0. \tag{1}$$

For the i-th element the radial rate is

$$V_{ri} = \frac{r - R_{i-1}}{R_i - R_{i-1}} V_{ii+1} + \frac{r - R_i}{R_{i-1} - R_i} V_{i-1i}, \quad i = \overline{1, N}. \tag{2}$$

Here R_i is the external radius of the i-th element ($R_0 = 0$); r is the flowing radial coordinate.

The rate of deformation of the i-th element is

$$e_{ri} = \frac{\partial V_{ri}}{\partial r}, \quad e_{\varphi i} = \frac{V_{ri}}{r}, \quad i = \overline{1, N}, \tag{3}$$

and the rates of change of its volume and shape

$$e_i = e_{ri} + 2e_{\varphi i}; \qquad \gamma_i = \frac{2}{3} | e_{\varphi i} - e_{ri} |, \quad i = \overline{1, N}. \tag{4}$$

In order to calculate the unknown flow rates according to the MPE scheme we use a variation principle. Assuming that the base material is linearly viscous, this principle is transformed to an extremum condition of the function

$$I = \int_{\vartheta} [\eta_0 (\varphi \gamma^2 + \psi e^2) + P_L e] \, d\vartheta \tag{5}$$

Institute of Materials Science Problems, Ukrainian Academy of Sciences, Kiev. Translated from Poroshkovaya Metallurgiya, No. 3(363), pp. 23-29, March, 1993. Original article submitted November 28, 1991.

1068-1302/93/3203-0208$12.50

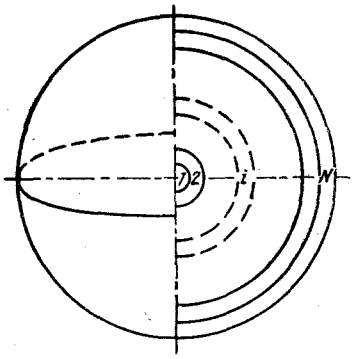

Fig. 1. Division of the porous material into permeable elements.

(ϑ = volume of the sphere). Differentiating (5) with respect to the flow rates and setting the derivatives equal to zero:

$$\frac{\partial I}{\partial V_{kk+1}} = 0, \quad k = \overline{1, N}. \tag{6}$$

To complete the system of linear equations (6) it is necessary to add condition (1).

We find the density field by using the law of mass conservation, which in the given case is written in a discrete form:

$$\frac{dM_i}{dt} - \frac{\rho_{i-1} + \rho_i}{2} S_{i-1} (V_{i-1i} - R_{i-1}) + \frac{\rho_{i+1} + \rho_i}{2} S_i (V_{ii+1} - R_i) = 0, \tag{7}$$

where M_i and ρ_i are the mass and density of the i-th element; S_i and R_i are the surface area and rate of displacement of the i-th sphere. In this case

$$S_i = 4\pi R_i^2, \tag{8}$$

$$M_i = \frac{4}{3} \pi (R_i^3 - R_{i-1}^3). \tag{9}$$

Substituting (8) and (9) in (7) we obtain

$$\rho_i = \frac{3}{2(R_i^3 - R_{i-1}^3)} \{\rho_{i-1} [R_{i-1}^2 (V_{i-1i} - R_{i-1})] + \rho_i [R_{i-1}^2 V_{i-1i} - R_i^2 V_{ii+1} - R_i^2 R_i + R_{i-1}^2 R_{i-1}] + \rho_{i+1} [R_i^2 (R_i - V_{ii+1})]\}, \quad i = \overline{1, N} \tag{10}$$

(we assume $\rho_0 = 0, \rho_{N+1} = 0$).

We select the rate of movement of the grid construct in such a way that in the solution of the homogeneous case flow between elements did not occur:

$$R_i = \frac{R_N}{N} i; \qquad R_i = \frac{V_{NN+1}}{N} i, \quad i = \overline{0, N} \tag{11}$$

(the grid is structured uniformly along the radius of the sphere). In order to complete the system (10), it is necessary to supplement it with an equation defining the unknown function R_N, which describes the change in the radius of the sphere with time:

$$R_N = V_{NN+1}. \tag{12}$$

The system of ordinary differential equations (10), (12) was solved numerically for the unknown functions ρ_i (i = 1, ..., N) and R_N using the fourth-order Runge–Kutta method installed in the calculation scheme with a "floating" step algorithm. The dimensionless parameter of a cycle $0 \le T \le 1$ defining a fraction of the total process time we chosen as the independent variable. The following physicomechanical properties of iron were used in carrying out the calculations: theoretical density ρ_K = 7800 kg/m^3, local Laplacian pressure P_{L_0} = 2.3 MPa [3], coefficient of viscosity $\eta_0 = 2.5 \cdot 10^5$ MPa·sec [4]. The dependence of the

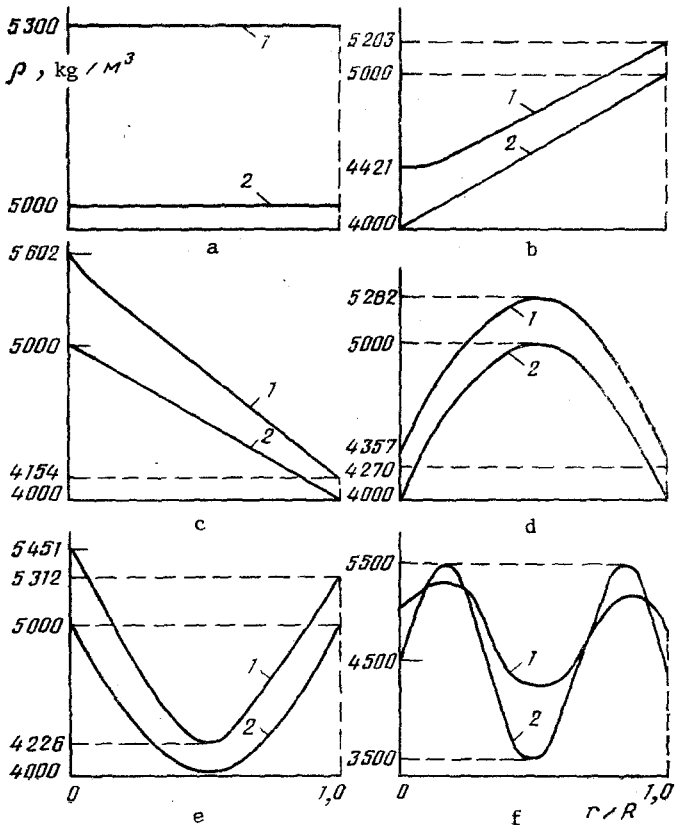

Fig. 2. Density distribution along the radius of the sphere (1) at the beginning of sintering, ρ_H; (2) at the end of sintering, ρ_K.

effective Laplacian pressure on porosity ([5], equation (16)) was allowed for in the calculation. The reduced time [5] was taken as $\tau_0 = 0.25$ (for the physicomechanical properties given above, this value corresponds to the sintering of porous iron for 10 h at 900°C). The number of layers selected was N = 10.

The results of the calculations for various initial conditions are shown in Fig. 2 in the form of curves of density distribution along the radius of the sphere at the beginning and end of sintering. Data for a "self test" of the model are shown in Fig. 2a. Here, for the initial condition of homogeneity, the density field remains uniform at all times in the heat treatment cycle, which agrees with known data for the structure of porous materials during sintering. Calculations were also carried out for density fields with initially linear (Fig. 2b, c), parabolic (Fig. 2d, e), and sinusoidal (Fig. 2f) distributions along the radius. The results show a tendency for the density gradient to decrease during sintering. However, under certain initial conditions the drop in porosity between individual segments may increase (Fig. 2c, d, e). Marked increase in the density in a zone near the center of the sphere is caused mainly by the existence of a discontinuity in the initial density distribution at the center, and also by the fact that the circumferential deformation in a spherical layer increases with decreasing radius [2].

Using the given mathematical model it is also possible to solve the problem of the sintering of a spherical layer with an internal constraint (Fig. 3), which is equivalent to sintering in the presence of a rigid inclusion.

Sintering of a Porous Cylinder with End Constraints under Uniaxial Compression. The porous cylinder is considered to be initially homogeneous. The rheological properties of the solid phase are linearly viscous. The method of finite elements is used to solve the problem [6]. The stress–deformation state of the porous cylinder is axially symmetric, and therefore its volume is divided into circular elements subdivided by a diagonal section into two elements having a triangular cross section (Fig. 4). Because of symmetry it is necessary to consider only half of the bar. We take as boundary conditions that on the lower face

$$V_z = 0, \quad V_r = 0 \tag{13}$$

and on the upper

$$V_z = -V_p, \quad V_r = 0 \tag{14}$$

(V_p is the velocity of the upper punch).

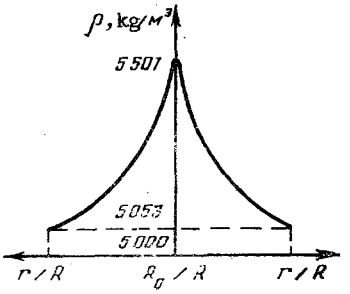

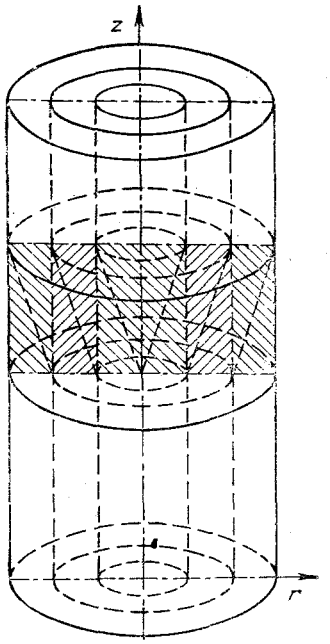

Fig. 3 Fig. 4

Fig. 3. Radial density distribution after sintering a spherical layer with an internal constraint.

Fig. 4. Method of division into elements for the axially symmetric problem.

In distinction from [5], where the problem was considered assuming uniform distributions of stress and density, we will investigate the effect of the boundary conditions and initial properties. An effect was found in [5] consisting of a decrease in the radial flow rate, and in certain cases (in [5] this is described by equation (27)) even a change in its direction. In this communication the various factors which influence the course of sintering are considered more fully, since the problem is solved by an extremum method. Therefore the number of possible outcomes is greater. However, as shown by the calculations, there are definite correlations between the results of the corresponding solutions for the homogeneous and extremum arrangements.

Figure 5 shows, schematically, the shape distortion and volume distribution of density in an article subjected to various rates of movement of an external punch. The physicomechanical properties of copper were used in the calculations: theoretical density ρ_K = 8940 kg/m^3, initial density of the bar ρ_H = 7000 kg/m^3, initial height of the cylinder h_H = 0.1 m, initial diameter d_H = 0.04 m. The reduced sintering time τ_0 = 0.75 corresponds to sintering porous copper for 45 min at 1050°C [7].

For $V_p = 10^{-5}$ m/sec (corresponding to a total punch travel Δh of 0.027 m in 45 min) condition (27) in [5] is not satisfied (Fig. 5a). The cylinder assumes a barrellike shape. In this case the density is a minimum in the central zones adjacent to the faces. The maximum density is attained in the corners formed by the contact and lateral surfaces of the bar. For $V_p = 3 \cdot 10^{-6}$ m/sec (total Punch travel Δh = 0.0081 m) condition (27) in [5] is satisfied throughout the entire process. In this case a "waist" forms (Fig. 5b). The minimum density occurs in the center of the bar, and the maximum in the central regions adjacent to the end faces. In this case sintering dominates over the effect of the external mechanical action. For $V_p = 5 \cdot 10^{-6}$ m/sec (total punch travel Δh = 0.0135 m) there exists a moment at which condition (26) in [5] is satisfied. When the tool moves at this rate a corrugation forms (Fig. 5c). The density field in this case is nearly uniform. A small increase in density is found in the equatorial region. The appearance of a corrugation may be explained as follows: at the beginning of the process a bulge forms whose density is lower than at the end faces. Consequently, the rate of shrinkage in this done becomes higher in the following periods of time. It should be noted that the formation of a corrugation depends also on the ratio of the initial height to the diameter of the bar: at h_N = 0.08 m, d_N = 0.04 m and similar initial values the formation of a corrugation was not observed (Fig. 5d).

Isothermal Sintering of a Porous Cylinder with a Nonuniform Density Distribution Caused by Previous Compaction. Figure 6a shows the density distribution in a porous cylindrical briquette after uniaxial compaction in a rigid die, calculated on the MPE [1] for the case of compaction of a bar of iron powder with an initial height to diameter ratio h_N/h_N = 2.0. The initial density was taken as 4000 kg/m^3, uniform throughout the volume, the coefficient of friction λ = 0.1, ratio of final and initial

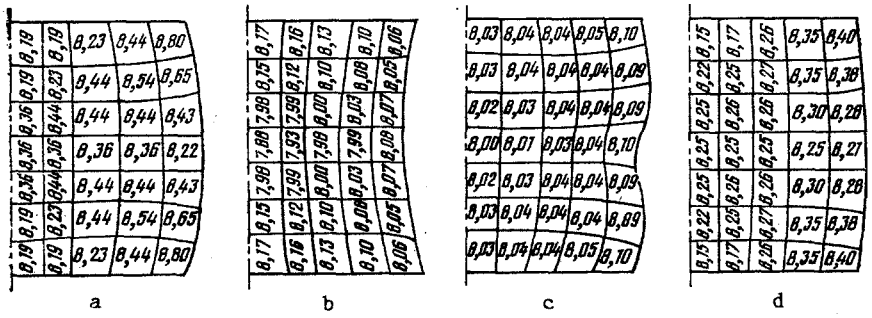

Fig. 5. Shape distortion and density (10^{-3} kg/m^3) distribution in a porous copper cylinder during sintering and compression with various rates of movement of the punch.

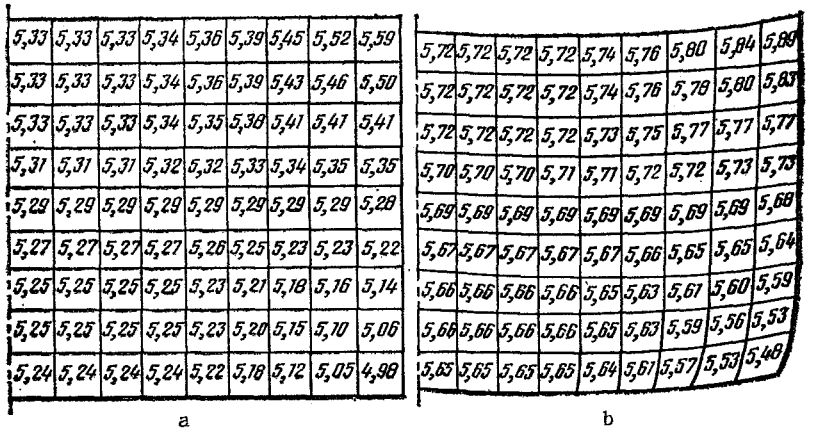

Fig. 6. (a) Density distribution (10^{-3} kg/m^3) in a porous cylindrical briquette after uniaxial compaction in a rigid die; (b) Shape distortion of and density distribution in the briquette after sintering.

heights $h_K/h_N = 0.75$. The solid phase was assumed to be elastic-plastic. The solution obtained agrees well with the results of [2, 4]. It is known that in the given case the density nonuniformity is caused exclusively by external friction. The upper peripheral regions of the briquette have the highest density (Fig. 6a). The density in the upper layer in contact with the punch increases from the center to the edge. The density in the layer at the base of the briquette is lower at the edge than at the center. This is due to the lower axial pressure in the layers adjacent to the die walls. The density decreases as the distance from the punch face increases.

The density field found by solution of the uniaxial compression problem is used as an initial condition in analyzing the sintering process. We use the finite element method [6] for this purpose. Neglecting gravitational and frictional forces, we take as boundary conditions:

$$V_{zm} = 0, \quad V_{rm} = 0, \tag{15}$$

where V_{zm} and V_{rm} are the axial and radial flow rates at the center of mass of the bar. The base material is considered to be linearly viscous; the reduced sintering time $\tau_0 = 0.25$. The distorted shape of the article and the density field after sintering are shown in Fig. 6b. The initial dimensions of the article correspond to the final dimensions after compression. The results are in good agreement with known experimental data [8, 9]. They confirm the empirically known fact that zones of increased porosity coincide with the directions of greatest shrinkage.

The information presented in Fig. 6, therefore, gives a complete picture of the industrial processing of a porous cylindrical bar, starting with compacting in a rigid die and ending with sintering.

LITERATURE CITED

1. E. A. Olevskii, M. B. Shtern, O. D. Serdyuk, et al., "Determination of the density field in a compacted article with a complicated shape by the method of permeable elements," Poroshk. Metall., No. 3, 15-21 (1989).
2. M. B. Shtern, G. G. Serdyuk, L. A. Maksimenko, et al., Phenomenological Theory of Powder Compaction [in Russian], Naukova Dumka, Kiev (1982).
3. V. V. Skorokhod, Rheological Principles of Sintering Theory [in Russian], Naukova Dumka, Kiev (1972).
4. I. M. Fedorchenko and R. A. Andrievskii, Principles of Powder Metallurgy [in Russian], Izd. Akad. Nauk USSR, Kiev (1961).
5. V. V. Skorokhod, E. A. Olevskii, and M. B. Shtern, "Continuum theory of sintering. I. Phenomenological model. Analysis of the effect of external forces on the kinetics of sintering," Poroshk. Metall., No. 1, 22-27 (1993).
6. O. Zenkevich, The Finite Element Method in Engineering [Russian translation], Mir (1975).
7. V. V. Skorokhod and S. M. Solonin, Physicometallurgical Principles of the Sintering of Powders [in Russian], Metallurgiya, Moscow (1984).
8. F. V. Lenel, H. H. Hausner, et al., Powder Metallurgy, No. 10, 190 (1962).
9. M. Mitkov, "Auswirkung der porenorientierung beilose peschuttetan gepressten kupterpulver auf die schrumptungsan-isotropic," 5th Eur. Symp. Powd. Met., Vol. 3, Stockholm (1978), pp. 379-386.